

University of Groningen

Energy Extraction of Pontoon-Type Wave Energy Converter

Tay, Zhi Yung; Wei, Yanji; Vakis, Antonis I.

Published in:

Proceedings of the 37th International Conference on Ocean, Offshore and Arctic Engineering

IMPORTANT NOTE: You are advised to consult the publisher's version (publisher's PDF) if you wish to cite from it. Please check the document version below.

Publication date:

2018

[Link to publication in University of Groningen/UMCG research database](#)

Citation for published version (APA):

Tay, Z. Y., Wei, Y., & Vakis, A. I. (2018). Energy Extraction of Pontoon-Type Wave Energy Converter. In *Proceedings of the 37th International Conference on Ocean, Offshore and Arctic Engineering ASME*.

Copyright

Other than for strictly personal use, it is not permitted to download or to forward/distribute the text or part of it without the consent of the author(s) and/or copyright holder(s), unless the work is under an open content license (like Creative Commons).

The publication may also be distributed here under the terms of Article 25fa of the Dutch Copyright Act, indicated by the "Taverne" license. More information can be found on the University of Groningen website: <https://www.rug.nl/library/open-access/self-archiving-pure/taverne-amendment>.

Take-down policy

If you believe that this document breaches copyright please contact us providing details, and we will remove access to the work immediately and investigate your claim.

Downloaded from the University of Groningen/UMCG research database (Pure): <http://www.rug.nl/research/portal>. For technical reasons the number of authors shown on this cover page is limited to 10 maximum.

ENERGY EXTRACTION OF PONTOON-TYPE WAVE ENERGY CONVERTER

Zhi Yung TAY

Engineering Cluster,
Singapore Institute of Technology,
10 Dover Drive, Singapore 138683.

Yanji WEI

Faculty of Science and Engineering,
University of Groningen,
Nijenborgh 4, Groningen,
9747AG the Netherlands.

Antonis I. VAKIS

Faculty of Science and Engineering,
University of Groningen,
Nijenborgh 4, Groningen,
9747AG the Netherlands.

ABSTRACT

Presented herein is the performance of a pontoon-type wave energy converter (WEC) similar to that of the 'Floater Blanket' WEC, which consists of a grid of interconnected floating elements. The current WEC design takes into account the elastic deformation of the structure under wave action and investigates its efficiency in generating wave energy as compared to its counterparts that achieve this via rigid body motions. The power take off (PTO) systems are installed at the seabed and attached to the WEC to generate energy via the vertical motions of the WEC's structural modules. Three types of pontoon-type WEC designs are investigated, i.e. with hinges, with a reduced number of hinges and without hinges. In addition, the influence of the flexibility of the structural modules towards the energy generation is also investigated in order to assess its performance when behaving like an elastic material. The pontoon-type WEC's structural modules with fewer or without hinge connections are preferable due to their ease in installation, while allowing for flexible deformation in the structural design would yield savings in material cost.

INTRODUCTION

Ocean wave energy is considered as a concentrated form of solar energy with an attractive feature of high energy density. However, systems to harvest utility-scale electrical power from ocean waves present a great challenge. Despite the large variation in concepts of wave energy

converters (WECs), there remains no clear consensus on the optimal designs. The cost, survivability, and power quality are the major obstacles.

The present work advocates a WEC design, seeking to overcome the current obstacles in wave energy technologies. The new idea, namely a pontoon-type wave energy converter (WEC), which is similar to the Ocean Grazer WEC [1-2], consists of a grid of interconnected floating elements, with each element being connected to an individual PTO unit. The major difference is that the current design takes into account the elastic deformation of the structure that may potentially increase its survivability and reduce its construction cost. An Ocean Grazer WEC consists of ten hinged floating elements has been investigated numerically via both time domain [3] and frequency domain models [4]. Their results demonstrated that a WEC system with multiple oscillators can efficiently extract wave energy over a broad range of energy-dense wave periods by adapting the configuration of oscillators. The limitation of these studies was that the floating elements were considered as rigid bodies and, therefore, the hydroelastic effects were omitted. It is thus interesting to investigate the influence of the flexibility of the structural modules towards the energy absorption.

Numerical modelling of pontoon-type WEC systems can borrow the established approaches from other offshore engineering fields, i.e. pontoon-type very large floating structures (VLFSs), in which hydroelastic effects are significantly important. A comprehensive literature survey on hydroelastic analysis of pontoon-type VLFS can be found in [5]. In those models, the VLFSs usually consist of multiple linked standardized modules. Each module is considered as an elastic (isotropic/orthotropic) thin plate

with free edges. For example, Gao *et al.* [6] adopted a modal expansion method to investigate the hydroelastic response of VLFS with a flexible line connection; Loukogeorgaki *et al.* [7] proposed a three-step numerical analysis to investigate the hydroelastic performance of a mat-shaped floating breakwater consists of a grid of flexible modules; Yoon *et al.* [8] investigated hydroelastic effects on floating plates with multiple hinge connections. Their results indicated that applying hinge and semi-rigid line connections can effectively reduce the hydroelastic response of the VLFS as well as the stress resultants. Their models can be easily extended for pontoon-type WEC investigation by adding a cluster of PTO forces into the motion equations.

The pontoon-type WEC is not the first WEC concept that takes into account the hydroelasticity. Several deformable WECs have been proposed recently, such as a piezoelectric WEC [9] and a rubber tube WEC [10], and researchers have developed the numerical and mathematical models to assess their performance. Renzi [11] developed a mathematical model of a submerged elastic plate with damping, in order to understand the hydroelectromechanical-coupled dynamics of a piezoelectric WEC. Babarit *et al.* [12] performed a numerical investigation on a tube WEC made of electroactive polymers. The model was simplified as a submerged elastic tube. The preliminary results showed very good agreement with the experiment. Another recent work by Tay [13] investigated the energy generation from an anti-motion device of VLFS by attaching a rotational PTO at the hinge. Although these new WEC concepts are still under investigation and require great research efforts, development of these models has improved the state-of-the-art of numerical modelling of WECs.

The present work focuses on the performance of a novel pontoon-type WEC when subjected to regular waves of different frequency. The effect of elastic deformation of the structure is taken into consideration in assessing the power generation of the WEC and these results are compared with their counterparts governed by the rigid body motion. In addition, the influence of the numbers of connected modules towards the power generation are also studied. The details of the cases considered in this paper are presented in the next section.

PROBLEM DEFINITION

Referring to Fig. 1, we consider N pontoon-type modules each with a length l , width B and depth D connected to each other by using $(N - 1)$ line hinge connectors. Each module is an isotropic elastic material with a Young's

modulus E and mass density ρ_p . The plate floats in a draft T_w and on a constant water depth of H . When connected together, the pontoon type WEC has a total length dimension $L = N \times l$, breadth B and depth D . A total constant M number of PTO systems, each with a constant PTO damping B_{PTO} , are installed at the seabed and attached to the WEC to generate energy via the vertical motions of the WEC's structural modules (see Fig. 1). The PTO system is spaced at an equal interval of $\frac{L}{12}$ in the horizontal direction (x - axis) and $\frac{B}{8}$ in the transverse direction (y - axis) as shown in Fig 1(A), therefore making a total number of $M = 99$ PTO systems as shown in Figs 1(A) to (C).

The pontoon-type WECs considered in this paper are shown in Table 1. Referring to Table 1, three groups of pontoon-type WECs, each with different L are considered. For each group of WEC, four types of WEC, i.e. Type-A, B, C and D, each with different numbers of modules N , are further considered and depicted in Figs. 1(A) to (D), respectively. It is to be noted that Type-A WEC has the highest number of line hinge connectors, whereas Type-B and C have a reduced number of line hinge connectors. The Type D pontoon-type WEC is a single module WEC and behaves like a continuous mat-like very large floating structures (VLFS). These different types of WECs are subjected to different elastic deformation behavior due to their different module length l and Young's modulus E , thus allowing the investigation of the effect of elastic deformation (i.e. structural elasticity) towards the performance of the WEC. In order to investigate the effect of structural elasticity towards the wave energy generation, two different E values are considered to demonstrate the elastic deformation and rigid body motion. Also, it is to be noted that the total number of PTO systems are kept the same ($M = 99$) for all the WECs considered here in order to ensure a fair comparison of the performance of the WECs.

The regular wave with a wave amplitude $2A$ and wave frequency ω is assumed to approach the WEC at the head sea direction. The structural, PTO system and wave properties considered in this paper are summarized in Table 1.

In order to facilitate the discussion, the pontoon-type WEC will be referred to by their Group and Types as summarized in Table 1. For example, a Group 1 – Type A WEC would refer to the pontoon-type WEC with $L = 120\text{m}$ and $N = 12$.

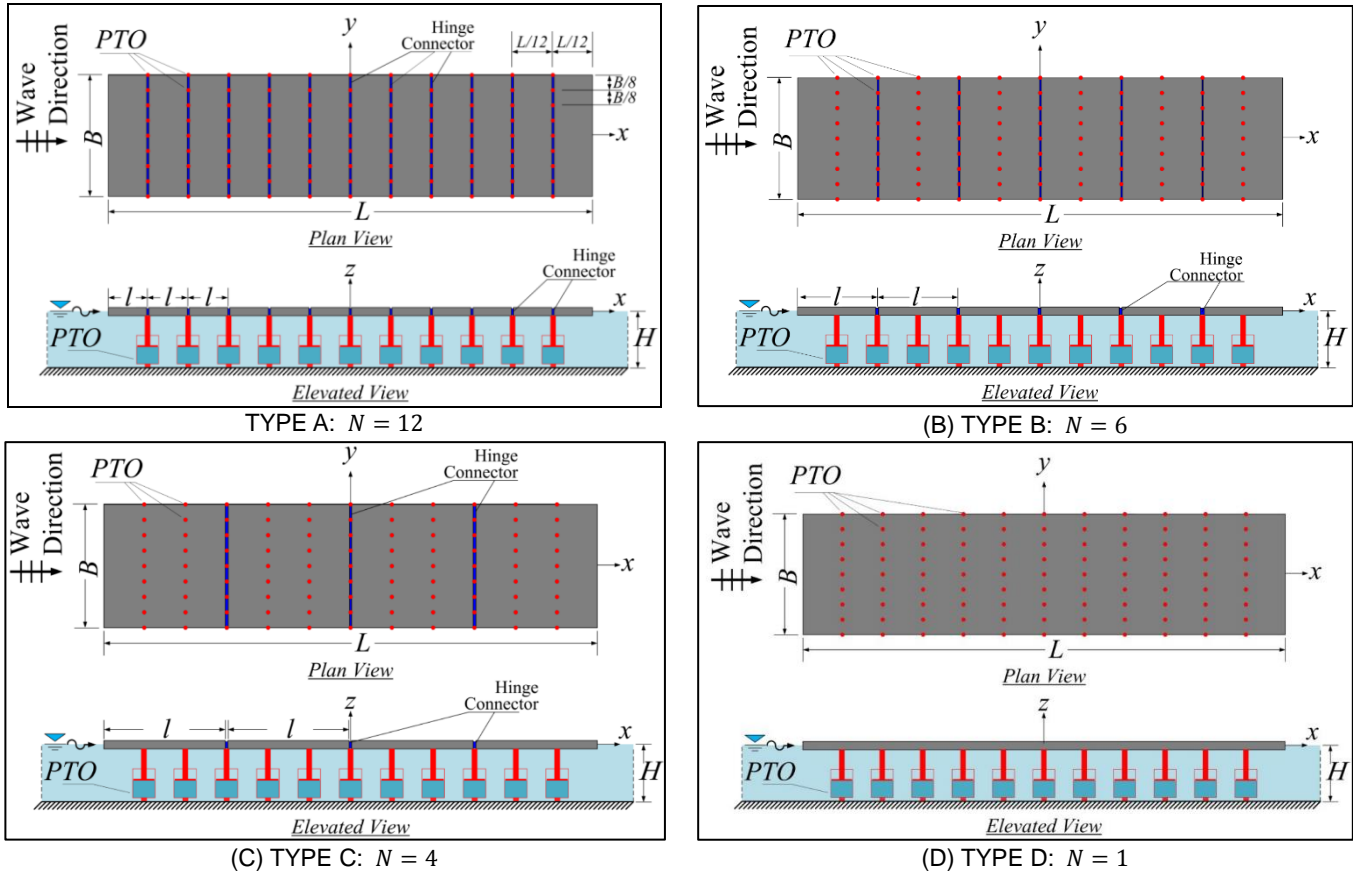


FIGURE 1 – PONTOON-TYPE WEC WITH (A) TYPE A: $N = 12$ MODULES (B) TYPE B: $N = 6$ MODULES (C) TYPE C: $N = 4$ MODULES (D) TYPE D: $N = 1$. $M = 99$ FOR ALL TYPES.

TABLE 1 – PROPERTIES FOR DIFFERENT CASES CONSIDERED

Group	Structural Properties									PTO System	Wave Properties	Water Depth H (m)
	L (m)	Type	N	E (GPa)	ρ_p ($\frac{kg}{m^3}$)	B (m)	D (m)	T_w (m)	M	$\frac{B_{PTO}}{m}$ ($\frac{MN \cdot s}{m}$)	ω ($\frac{rad}{s}$)	
1	120	A B C D	12 6 4 1	0.2 & 200	512.5	30	2	1	99	180	0.1 to 1.6 (0.025 interval)	600
2	240	A B C D	12 6 4 1									
3	360	A B C D	12 6 4 1									

MATHEMATICAL FORMULATION

Assumptions for Water-Structure Model

Water Domain The usual assumption that the water is a real fluid based on potential theory is applied here, where the water is assumed to be inviscid, incompressible and its flow is irrotational. Based on these assumptions, the fluid

motion may be represented by a velocity potential $\Phi(x, y, z, t)$. We consider the water to oscillate in a steady-state harmonic motion with the circular frequency $\omega = 2\pi/T$. The velocity potential $\Phi(x, y, z, t)$ could be expressed into the following form

$$\Phi(x, y, z, t) = \text{Re}\{\phi(x, y, z)e^{-i\omega t}\} \quad (1)$$

The single frequency velocity potential $\phi(x, y, z)$ must satisfy the Laplace equation (2) [14] and the boundary conditions on the surfaces as shown in Fig. 1.

$$\nabla^2 \phi = 0 \quad \text{in } \Omega \quad (2)$$

These boundary conditions are given as follows [14]:

$$\frac{\partial \phi}{\partial z} = i\omega w \quad \text{on } S_{HB} \quad (3)$$

$$\frac{\partial \phi}{\partial n} = 0 \quad \text{on } S_{HS} \quad (4)$$

$$\frac{\partial \phi}{\partial z} = \omega^2 \phi \quad \text{on } S_F \quad (5)$$

$$\frac{\partial \phi}{\partial z} = 0 \quad \text{on } S_B \quad (6)$$

where n is the unit normal vector to the surface S . The wave velocity potential must also satisfy the Sommerfield radiation condition at the artificial fluid boundary at infinity S_∞ as $|(x, y) \rightarrow \infty|$ [14].

$$\lim_{|(x, y) \rightarrow \infty|} \sqrt{|(x, y)|} \left(\frac{\partial}{\partial |(x, y)|} - ik \right) (\phi - \phi_{in}) = 0 \quad \text{on } S_\infty \quad (7)$$

where k and ϕ_{in} are the standard wave number and incident velocity potential as found in [15].

The Laplace equation (2) together with the boundary conditions (2) to (7) on the surface S are transformed into a boundary integral equation (BIE) by using the Green's 2nd Theorem via a free surface Green's function given in [6] that satisfies the surface boundary condition at the free water surface S_F , the seabed S_B and at infinity S_∞ . Hence, only the wetted surface of the side and bottom of the floating body, S_{HS} and S_{HB} , respectively, need to be discretised into panels so that the boundary element method could be used to solve for the diffracted and radiated potential. For details on the Green's function used in solving the BIE, refer to [6, 15].

Structure Domain The pontoon-type WEC on the other hand is modelled as a solid plate with thickness h by using the Mindlin thick plate theory [16-18]. The solid plate is assumed to be perfectly flat with free edges and the plate material is commonly assumed to be isotropic and obeys Hooke's Law. Similar to a VLFS, the structure is moored on site by a station keeping system and is restrained from moving in the horizontal x - y plane directions and only allowed to move vertically. Hence, the motion of the WEC could be described by the deflection $w(x, y)$, the rotation about the y -axis $\psi_x(x, y)$ and the rotation about the x -axis $\psi_y(x, y)$ as follows:

$$\kappa^2 Gh \left[\left(\frac{\partial^2 w}{\partial x^2} + \frac{\partial^2 w}{\partial y^2} \right) + \left(\frac{\partial \psi_x}{\partial x} + \frac{\partial \psi_y}{\partial y} \right) \right] + \rho_p h \omega^2 w = p(x, y) \quad (8)$$

$$D \left[\frac{(1-\nu)}{2} \left(\frac{\partial^2 \psi_x}{\partial x^2} + \frac{\partial^2 \psi_y}{\partial y^2} \right) + \frac{(1+\nu)}{2} \left(\frac{\partial^2 \psi_x}{\partial x^2} + \frac{\partial^2 \psi_y}{\partial x \partial y} \right) \right] - \kappa^2 Gh \left(\frac{\partial w}{\partial x} + \psi_x \right) + \rho_p \frac{h^3}{12} \omega^2 \psi_x = 0 \quad (9)$$

$$D \left[\frac{(1-\nu)}{2} \left(\frac{\partial^2 \psi_y}{\partial y^2} + \frac{\partial^2 \psi_x}{\partial x^2} \right) + \frac{(1+\nu)}{2} \left(\frac{\partial^2 \psi_y}{\partial y^2} + \frac{\partial^2 \psi_x}{\partial x \partial y} \right) \right] - \kappa^2 Gh \left(\frac{\partial w}{\partial y} + \psi_y \right) + \rho_p \frac{h^3}{12} \omega^2 \psi_y = 0 \quad (10)$$

where $G = E/[2(1+\nu)]$ is the shear modulus, κ^2 the shear correction factor taken as 5/6 [19], ρ_p the mass density of the plate, h the thickness of the plate, $D = Eh^3/[12(1-\nu^2)]$ the flexural rigidity, E the Young's modulus and ν the Poisson ratio. The pressure $p(x, y)$ in Eq. (8) comprises the hydrostatic and hydrodynamic pressure. The boundary conditions at the free edges of the floating plate are

$$M_{nn} = D \left[\frac{\partial \psi_n}{\partial n} + \nu \frac{\partial \psi_s}{\partial s} \right] = 0 \quad (11)$$

$$M_{ns} = D \left[\frac{(1-\nu)}{2} \right] \left[\frac{\partial \psi_n}{\partial s} + \frac{\partial \psi_s}{\partial n} \right] = 0 \quad (12)$$

$$Q_n = \kappa^2 Gh \left[\frac{\partial w}{\partial n} + \psi_n \right] = 0 \quad (13)$$

where M_{nn} , M_{ns} and Q_n are the bending moment, twisting moment and shear force, respectively. s and n denote the tangential and normal directions to the section of the plate, respectively.

It is to be noted that the articulated plate anti-motion device is also modelled as a solid plate subjected to the same governing equations (8) to (10) and boundary conditions (11) to (13).

Continuity Equations for Hinge Connector with PTO System

The interconnected WEC modules are hinged as shown in Fig. 1. The continuity equations for the interconnected plate at the hinge connector with PTO damping B_{PTO} located at $x_c = 0$ are

$$w|_{x=x_c^-} = w|_{x=x_c^+} \quad (14)$$

$$\psi_y|_{x=x_c^-} = \psi_y|_{x=x_c^+} \quad (15)$$

$$M_x|_{x=x_c^-} = M_x|_{x=x_c^+} = 0 \quad (16)$$

$$M_{xy}|_{x=x_c^-} = M_{xy}|_{x=x_c^+} = 0 \quad (17)$$

$$Q_x|_{x=x_c^-} = Q_x|_{x=x_c^+} = 0 \quad (18)$$

These continuity requirements can be implemented into plate elements along the line connection using the standard finite element method.

The power take-off (PTO) system is attached at the connector to convert the kinetic energy of the interconnected plate due to wave action to stored potential energy. This is modelled as damper along the line hinge connector, i.e. y -axis at $x = 0$ with PTO damping value B_{PTO} .

Equation of Motion for Water-Plate Model

The coupled water-structure problem is solved by using the coupled boundary element-finite element scheme, where the Laplace equation together with the water boundary conditions are solved using the boundary element method whereas the plate equation and its boundary conditions using the finite element method. Due to space constraints, details of the solution scheme are not presented here, but interested readers can refer to these details in [15]. By using the modal expansion method for the plate deflections, the decoupled equation of motion of the water-structure problem can be written as

$$\left[-\omega^2(M + M_a) - i\omega(B_a + B_{PTO}) + (K_f + K_s + K_{rf}) \right] \bar{w} = F_e \quad (19)$$

where $\bar{w} = (w, \psi_x^-, \psi_x^+, \psi_y^-, \psi_y^+)$, M is the mass, K_f the flexural stiffness, K_s the shear stiffness and K_{rf} the restoring force. The added mass M_a , radiated damping B_a and exciting force can be found in [6] and will not be presented here due to its lengthy derivation. The equations can be further transformed into the matrix form to be solved using the finite element method. The typical B_{PTO} matrix of an interconnected node in the hinge connector is presented as follow

$$\mathbf{B}_{PTO} = \begin{matrix} & w & \psi_x^- & \psi_x^+ & \psi_y^- & \psi_y^+ \\ \begin{matrix} w \\ \psi_x^- \\ \psi_x^+ \\ \psi_y^- \\ \psi_y^+ \end{matrix} & \begin{bmatrix} 0 & 0 & 0 & 0 & 0 \\ 0 & 0 & 0 & 0 & 0 \\ 0 & 0 & 0 & 0 & 0 \\ 0 & 0 & 0 & +B_{PTO} & -B_{PTO} \\ 0 & 0 & 0 & -B_{PTO} & +B_{PTO} \end{bmatrix} \end{matrix} \quad (20)$$

It is noted here that for each node along the line connector, there will be five degrees of freedom, namely w , ψ_x^+ , ψ_x^- , ψ_y^- and ψ_y^+ . The positive (+) and negative (-) signs denote the right hand side and left hand side of the node in the line connector.

Generated Power from Anti-Motion Device

The vertical motion of the structural displacement w calculated from (19) can be used to compute the generated power P_a using Eq. (21) [20]

$$P_a = \frac{1}{2} \omega^2 B_{PTO} w^2 \quad (21)$$

The generated power P_a is then expressed as capture width CW (see Eq. 22) by normalising with the wave power resource $P_{resource}$ in order to quantify the efficiency of the anti-motion device in generating wave energy.

$$CW = \frac{P_a}{P_{resource}} \quad (22)$$

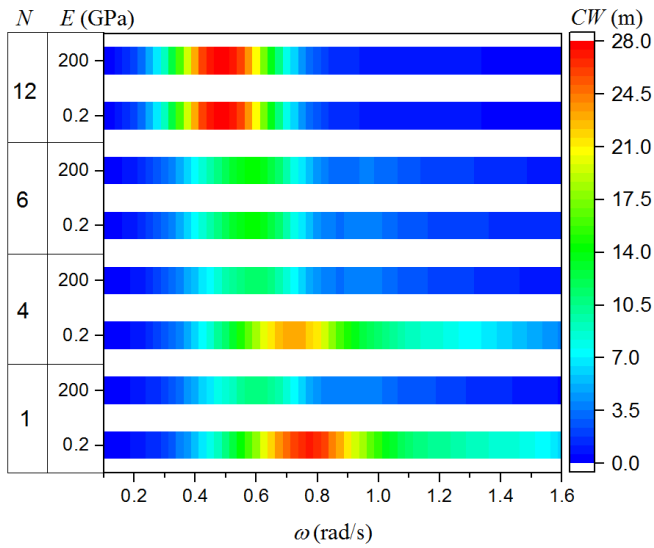
The CW has to be as large as possible for the WEC to be effective in generating wave energy. The wave power resource $P_{resource}$ in (22) is given as [21]

$$P_{resource} = \frac{\rho g^2 T H^2}{64\pi} \quad (23)$$

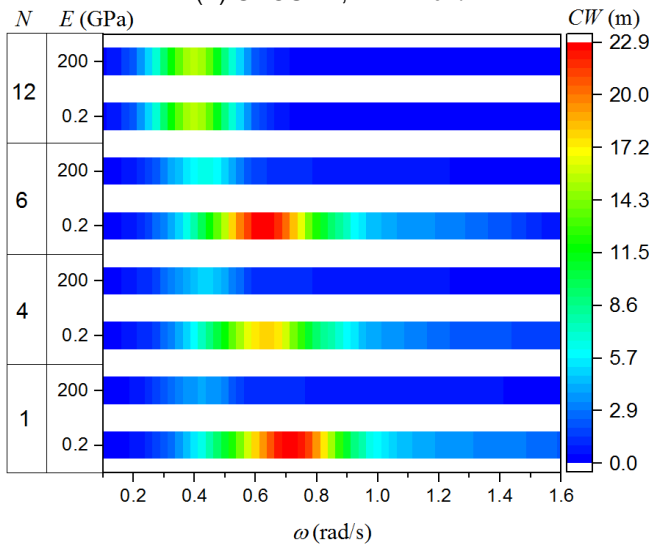
where ρ is the mass density of sea water, g the gravitational acceleration, T the wave period and H the significant wave height.

RESULTS AND DISCUSSION

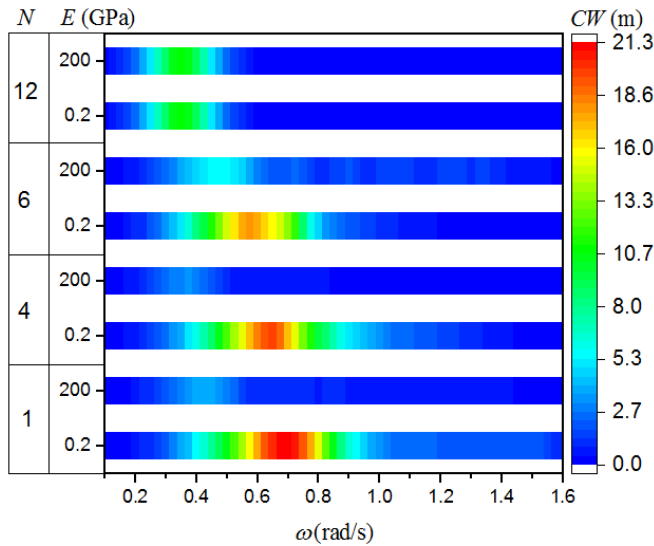
Figure 2 shows the capture width for Group 1, 2 and 3 pontoon-type WECs when subjected to regular waves of wave frequency ω ranging from 0.1 to 1.6 rad/s. For each group of pontoon-type WEC considered in Fig. 2, the capture width of the WECs with different N values are further compared, where $N = 12, 6, 4$ and 1 correspond to Type-A, B, C and D as summarized in Table 1. In addition to that, two different Young's Moduli E are considered to investigate the effect of rigidity towards the performance of the WECs. By focusing on the Group 1 pontoon-type WEC where $L = 120m$, the results in Fig. 2(A) show that the CW of the WECs is the same when $N = 12$ and 6 for different E values. However, there is a significant difference in the CW between $E = 0.2GPa$ and $200GPa$ as N reduces to 4 and 1 , with the case with smaller E having a larger CW value, thus suggesting that the deformation of the pontoon-type WECs contributes to greater power generation. It is to be noted that the effect of E is significant here only when N is reduced, as a smaller value of N translates to each individual module having a longer l (see Fig. 1) and hence greater structure deformation under wave action. Likewise, similar results could be observed in Fig. 1(B) and 1(C) for $L = 240m$ and $360m$, respectively. It can also be seen clearly that in Figs. 1(B) and 1(C), the effect of structure deformation towards the CW is obvious even when $N = 6$, due to the larger l for each individual module being connected in the pontoon-type WEC.



(A) GROUP 1, $L = 120m$



(B) GROUP 2, $L = 240m$



(C) GROUP 3, $L = 360m$

FIGURE 2 – CAPTURE WIDTH FOR GROUP 1, 2 AND 3 PONTON-TYPE WECs

By only comparing the CW across Figs. 2(A) to (C) for $E = 200GPa$, it can be seen that the CW increases with the increase of N , suggesting that more energy could be generated when multiple modules are hinged together. However, it is possible to generate greater energy from the structural deformation of each individual module even when N is small (see for example, Fig. 1(B) and (C), when $N = 1, 4$ and 6, where CW is greater when $E = 0.2GPa$). It is interesting to note that when N becomes smaller, it is possible to generate greater energy from the flexible pontoon-type WEC as compared to their counterparts with more connectors. This finding denotes a significant savings cost due to shorter installation time and connector numbers as well as material cost. This is due to the fact that the WEC could be manufactured with less material to allow for flexible deformation provided that the stress resultants on the structure are within the stipulated allowable stress values to ensure safety and robustness.

Similar trends could be observed when the power absorbed P_a by the pontoon-type WEC is plotted in Fig. 3. The values of P_a in Fig. 3 are obtained by multiplying the CW obtained in Fig. 2 with the wave power resource $P_{resource}$ (22).

In order to clearly observe the influence of rigidity towards the P_a of the WECs, Fig. 4 is plotted to show only the WECs when the influence of E towards P_a is obvious. The black line denotes WECs with $E = 0.2GPa$ whereas the blue line denotes WECs with $E = 200GPa$. It can be seen clearly that the flexible deformation of the WEC, i.e. $E = 0.2GPa$ results in a significantly larger P_a value as compared to their rigid counterparts. The highest value of P_a for flexible pontoon-type WEC is found to be shifted to a higher frequency as compared to its counterpart of the rigid pontoon-type WEC. This shows that the flexible pontoon-type WEC is able to generate greater energy when excited at its higher order vibration modes. This phenomenon is evidenced from Fig. 5 that shows the maximum deflection taken along the centerline of the pontoon-type WEC when excited at its peak frequency. By comparing the deformation of the flexible pontoon-type WEC, it can be seen that the WEC that deforms in higher order vibration modes corresponds to higher P_a as shown in Fig. 4. For example, the case when $N = 6$ in Fig. 5(B) has a higher P_a due to the WEC deforming elastically at its higher order vibration modes. This results in more energy being generated from the elastic deformation of the structure.

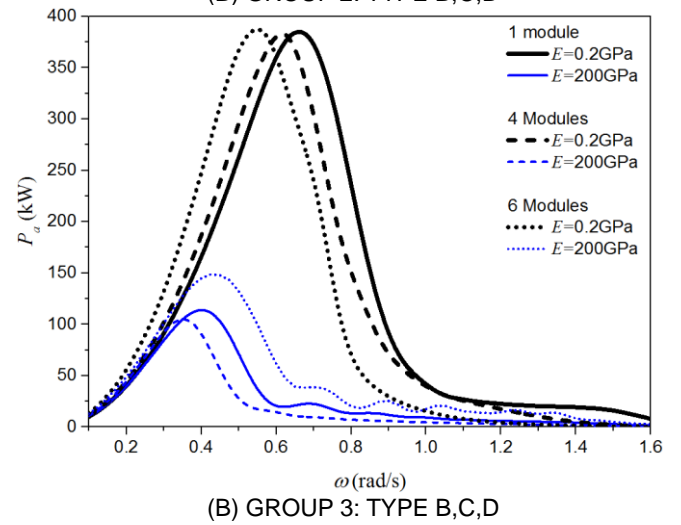
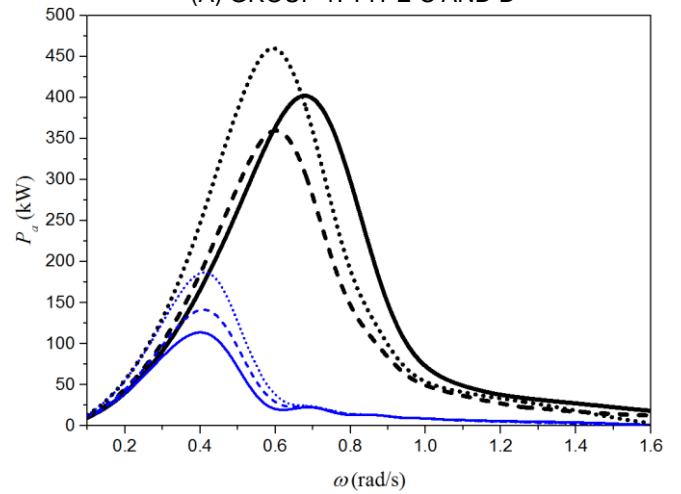
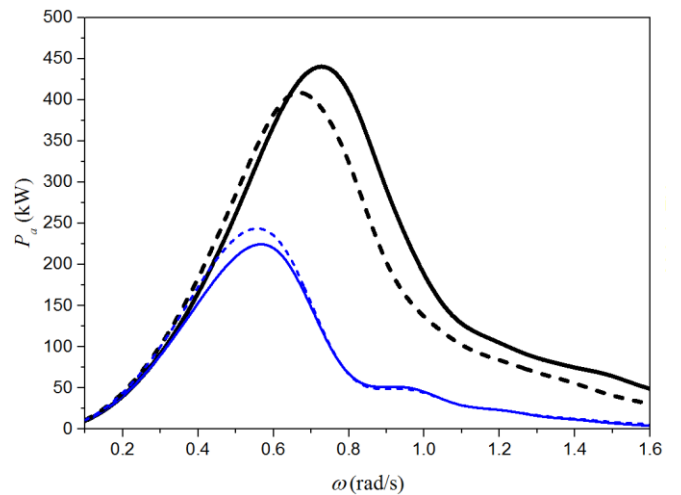
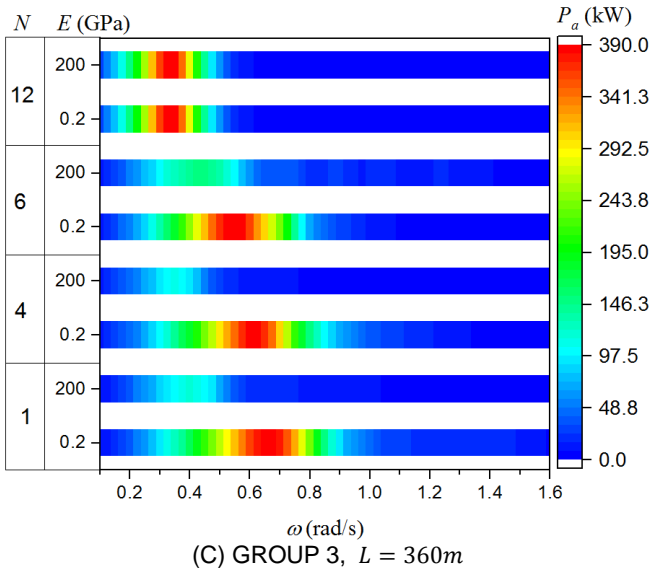
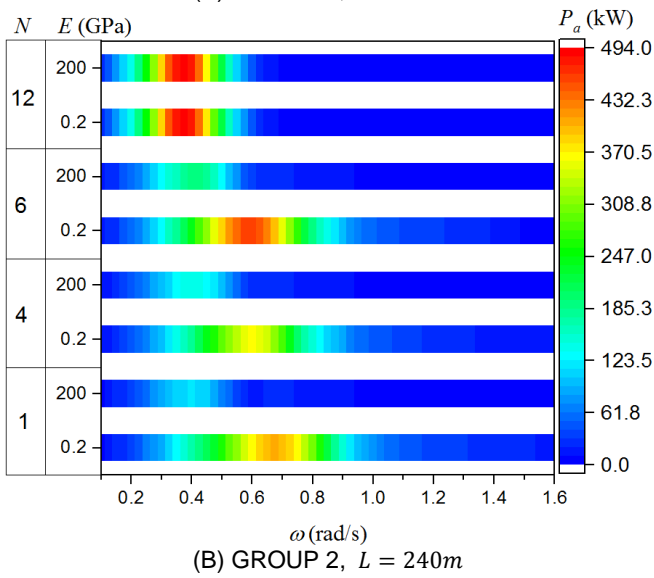
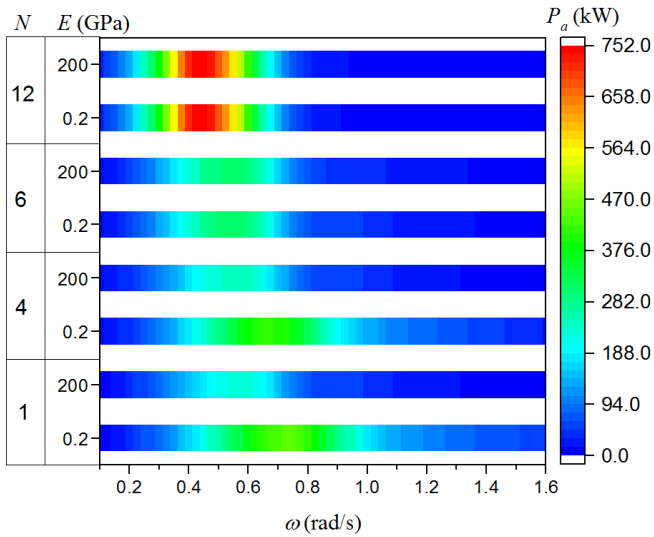
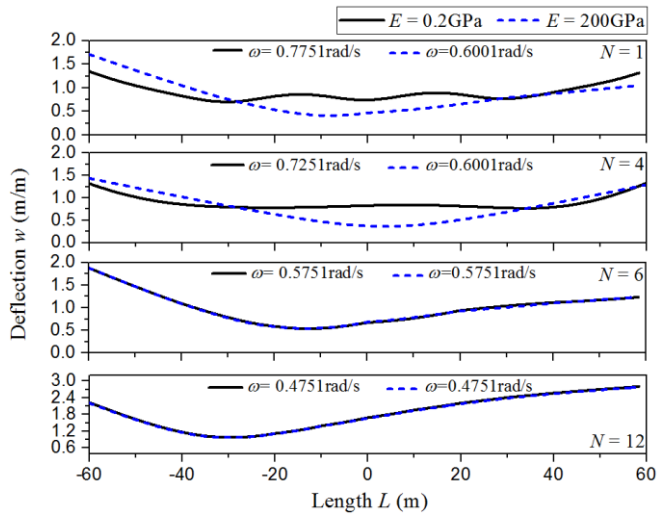
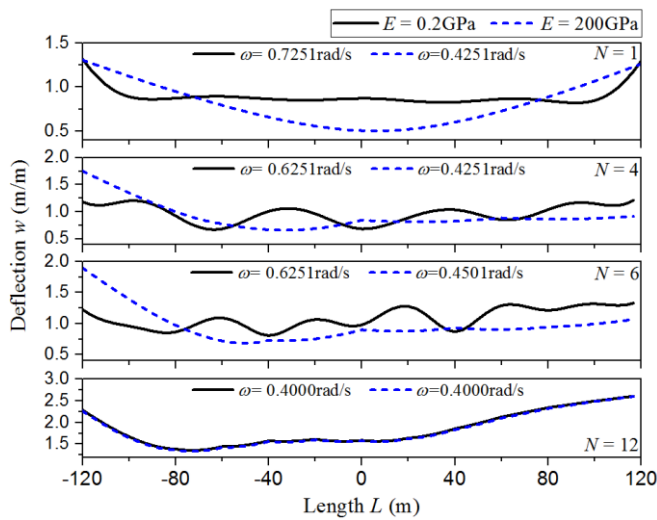


FIGURE 4 – COMPARISON OF POWER ABSORBED BETWEEN WEC WITH DIFFERENT RIGIDITY

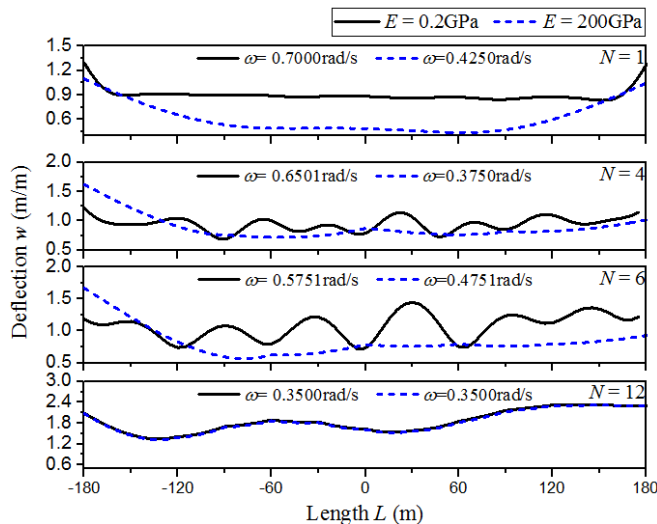
FIGURE 3 – POWER ABSORBED FOR GROUP 1, 2 AND 3 PONTOON-TYPE WECS



(A) GROUP 1: $L = 120m$



(B) GROUP 2: $L = 240m$



(C) GROUP 3: $L = 360m$

FIGURE 5 – COMPARISON OF MAXIMUM DEFLECTION OF PONTOON-TYPE WECs FOR GROUP 1, 2 AND 3 FOR DIFFERENT YOUNG'S MODULUS

CONCLUSIONS

This paper presents the performance of a novel pontoon-type WEC that utilizes its elastic deformation behavior in generating electricity from wave energy. The capture width and power absorbed of the pontoon-type WEC under the influence of different structure lengths, number of hinge connectors and rigidity are investigated. It was shown that more energy could be generated when the pontoon-type WEC motion is governed by its hydroelastic response as compared to its rigid body motion. In some cases, it was found that the flexible (smaller E) pontoon-type WECs with fewer hinge connectors are able to generate greater energy as compared to their rigid counterparts with higher number of hinge connectors. This significant finding indicates that substantial cost savings could be achieved as less material and fewer connectors are needed in the design of the pontoon-type WEC, which, at the same time, is able to generate greater energy. In addition to that, a smaller amount of hinge connectors can facilitate easier installation of pontoon-type WECs. For future work, the performance of the pontoon-type WEC under random wave conditions has to be considered and the uniform PTO configuration applied in the present pontoon-type WEC, which could be further optimized using optimization schemes such as the genetic algorithm method [22].

REFERENCES

- [1] Vakis, AI and Anagnostopoulos, JS, "Mechanical design and modeling of a single-piston pump for the novel power take-off system of a wave energy converter", *Renewable Energy*, vol.96, pp. 531-547, 2016.
- [2] Wang, C and Tay, Z, "Very large floating structures: applications, research and development", *Procedia Engineering*, vol.14, pp. 62-72, 2011.
- [3] Wei, Y, Barradas-Berglind, JJ, van Rooij, M, Prins, WA, Jayawardhana, B, and Vakis, AI, "Investigating the adaptability of the multi-pump multi-piston power take-off system for a novel wave energy converter", *Renewable Energy*, vol.111, pp. 598-610, 2017.
- [4] Wei, Y, Barradas Berglind, J, van Rooij, M, Prins, W, Jayawardhana, B, and Vakis, A, *A Frequency-Domain Model for a Novel Wave Energy Converter*, in *Proceedings of the Twelfth European Wave and Tidal Energy Conference*, Lewis, A, Editor 2017: University College Cork, Ireland. p. 657-1--657-8.
- [5] Watanabe, E, Utsunomiya, T, and Wang, CM, "Hydroelastic analysis of pontoon-type VLFS: A literature survey", *Engineering Structures*, vol.26, pp. 245-256, 2004.
- [6] Gao, RP, Tay, ZY, Wang, CM, and Koh, CG, "Hydroelastic response of very large floating structure with a flexible line connection", *Ocean Engineering*, vol.38(17), pp. 1957-1966, 2011.
- [7] Loukogeorgaki, E, Michailides, C, and Angelides, DC, "Hydroelastic analysis of a flexible mat-shaped floating breakwater under oblique wave action", *Journal of Fluids and Structures*, vol.31, pp. 103-124, 2012.
- [8] Yoon, JS, Cho, SP, Jiwinangun, RG, and Lee, PS, "Hydroelastic analysis of floating plates with multiple

- hinge connections in regular waves", *Marine Structures*, vol.36, pp. 65-87, 2014.
- [9] Jbaily, A and Yeung, RW, *Piezoelectric devices for ocean energy: a brief survey*, in *Journal of Ocean Engineering and Marine Energy* 2015. p. 101-118.
- [10] Farley, FJM, Rainey, RCT, and Chaplin, JR, "Rubber tubes in the sea", *Philosophical Transactions of the Royal Society A: Mathematical, Physical and Engineering Sciences*, vol.370, pp. 381-402, 2012.
- [11] Renzi, E, "Hydroelectromechanical modelling of a piezoelectric wave energy converter", *Proceedings of the Royal Society*, vol.472, 2016.
- [12] Babarit, A, Singh, J, Mélis, C, Watez, A, and Jean, P, "A linear numerical model for analysing the hydroelastic response of a flexible electroactive wave energy converter", *Journal of Fluids and Structures*, vol.74, pp. 356 - 384, 2017.
- [13] Tay, ZY, *Energy Generation from Anti-Motion Device of Very Large Floating Structure*, in *Proceedings of the Twelfth European Wave and Tidal Energy Conference*, Lewis, A, Editor 2017: University College Cork, Ireland. p. 674-1--674-9.
- [14] Faltinsen, OM. *Sea Loads on Ships and Offshore Structures*. Vol. 1, Cambridge University Press, UK, 1993.
- [15] Wang, CM and Tay, ZY. *Hydroelastic analysis and response of pontoon-type very large floating structures*. Fluid structure interaction II. Springer, 2011.
- [16] Tay, ZY. *Hydroelastic responses and interactions of mega floating fuel storage modules*. National University of Singapore, 2009.
- [17] Tay, ZY, Wang, CD, and Wang, CM, "Hydroelastic response of a box-like floating fuel storage module modeled using non-conforming quadratic-serendipity Mindlin plate element", *Engineering Structures*, vol.29(12), pp. 3503-3514, 2007.
- [18] Tay, ZY, Wang, CM, and Utsunomiya, T, "Hydroelastic responses and interactions of floating fuel storage modules placed side-by-side with floating breakwaters", *Marine Structures*, vol.22(3), pp. 633-658, 2009.
- [19] Wang, C, Reddy, JN, and Lee, K. *Shear deformable beams and plates: Relationships with classical solutions*. Elsevier, 2000.
- [20] Tay, ZY and Venugopal, V, "Hydrodynamic interactions of oscillating wave surge converters in an array under random sea state", *Ocean Engineering*, vol.145, pp. 382-394, 2017.
- [21] Goda, Y. *Random Seas and Design of Maritime Structures*. World Scientific, Singapore, 2010.
- [22] Tay, ZY and Venugopal, V, "Optimization of Spacing for Oscillating Wave Surge Converter Arrays Using Genetic Algorithm", *Journal of Waterway, Port, Coastal, and Ocean Engineering*, vol.143(2), pp. 04016019, 2016.